Free Radical Research, November–December 2011; 45(11–12): 1307–1324

informa
healthcare

ORIGINAL ARTICLE

Silibinin induced-autophagic and apoptotic death is associated with an increase in reactive oxygen and nitrogen species in HeLa cells

SIMIAO FAN[1], LIHUA LI[1], SHENGENG CHEN[1], YANG YU[1], MIN QI[1], SHIN-ICHI TASHIRO[2], SATOSHI ONODERA[2] & TAKASHI IKEJIMA[1]

[1]*China–Japan Research Institute of Medical and Pharmaceutical Sciences, Shenyang Pharmaceutical University; Shenyang 110016, China, and* [2]*Department of Clinical and Biomedical Sciences, Showa Pharmaceutical University; Tokyo 194-8543, Japan*

(Received date: 9 May 2011; Accepted date: 23 August 2011)

Abstract

Silibinin, as the major active constituent of silymarin, has its various biological effects. Here, we investigated the inhibitory effects of silibinin on HeLa cell growth in relation to autophagy and apoptosis induced by reactive oxygen species (ROS) and reactive nitrogen species (RNS) generation. Silibinin dose and time-dependently decreased cell growth cultured in medium containing 10% fetal bovine serum or in serum free media (SFM) with an IC_{50} of approximately 80–100 and 40–60 μM at 24 h, respectively. Silibinin induced autophagy at 12 h, confirmed by monodansylcadervarine (MDC) staining and up-regulation of beclin-1, and induced apoptosis at 24 h, detected by observation of apoptotic bodies and activation of caspase-3. 3-methyladenine (3-MA) inhibited silibinin-induced autophagy and attenuated the silibinin's inhibitory effect on cell viability, suggesting that autophagy enhanced silibinin-induced cell death. Silibinin increased ROS levels at 12 h, and ROS scavenger, *N*-acetylcysteine (NAC), significantly reversed the cytotoxicity of silibinin through inhibiting both autophagy and apoptosis. Specific antioxidants were applied and results indicated that hydroxyl radical (·OH) was the major ROS induced by silibinin, and OH scavenger glutathione (GSH) inhibited apoptosis and autophagy. Silibinin also generated RNS production in the cells at 12 h. High concentration of N omega-nitro-l-arginine methyl ester (L-NAME) as nitric oxide synthase (NOS) inhibitor attenuated the cytotoxicity of silibinin by decreasing ROS levels, leading to down-regulation of apoptosis. Silibinin also could interrupt the respiring functions of mitochondria, leading to ROS production and oxidative damage.

Keywords: *silibinin, HeLa cells, OH, GSH, L-NAME*

Introduction

Silibinin, also known as silybin, is the major active constituent of silymarin, the mixture of flavonolignans extracted from blessed milk thistle (*Silybum marianum*). Both *in vitro* and animal studies show that silibinin has hepatoprotective (antihepatotoxic) properties[1–3]. Silibinin also has anti-cancer effects against human prostate adenocarcinoma, estrogen-dependent and -independent breast carcinoma, ectocervical carcinoma, colon cancer and both small and nonsmall lung carcinoma cells[4–8]. Our previous researches demonstrated that silibinin exhibited anti-apoptotic effect on isoproterenol-treated rat cardiac myocytes by decreased expression of NO and inducible nitric oxide synthase (iNOS) [9] and by increased superoxide dismutase (SOD) activity [10]. Silibinin was also found to promote cell protective superoxide anion (O_2^-) production in human breast cancer MCF-7 cells and exogenous SOD markedly enhanced silibinin-induced apoptosis [11]. Silibinin induced reactive oxygen species (ROS) and reactive nitrogen species (RNS) generation and there existed an inter-regulation pattern between RNS and ROS in human breast carcinoma MCF-7 cells [12]. In human fibrosarcoma HT1080 cells, silibinin displayed cytotoxic effect through a reactive oxygen species pathway and hydrogen peroxide (H_2O_2) was the major responsive ROS [13]. In this study, silibinin induced autophagic and apoptotic death in HeLa cells through induction of ROS and RNS generation.

Correspondence: Takashi Ikejima, China-Japan Research Institute of Medical and Pharmaceutical Sciences, Shenyang Pharmaceutical University, 103 Wenhua Road, 110016 Shenyang, Liaoning, P. R. China. Tel/Fax: +86-24-2384-4463. E-mail: ikejimat@vip.sina.com

ISSN 1071-5762 print/ISSN 1029-2470 online
DOI: 10.3109/10715762.2011.618186

ROS include O_2^-, H_2O_2 and OH. ROS regulate many important cellular events including transcription factor activation, gene expression, cell differentiation and proliferation [14]. ROS is generated as a natural byproduct of cellular metabolism, primarily in the mitochondria. Under normal conditions, ROS were balanced by cell's antioxidant defence systems. However, under environmental stress, ROS levels increased dramatically. This might result in significant insult to cellular structures. ROS cause tissue damage by reacting with lipids in cellular membranes, nucleotides in DNA and sulphydryl groups in proteins [15].

RNS such as nitrosonium cation (NO^+), nitroxyl anion (NO^-) or peroxynitrite ($ONOO^-$) are a family of antimicrobial molecules derived from nitric oxide ($\cdot NO$) and O_2^- produced by the enzymatic activities of inducible nitric oxide synthase 2 (NOS2) and NADPH oxidase. RNS acting together with ROS cause cell damage, therefore, these two species are often collectively referred to as ROS/RNS [16].

Autophagy, or autophagocytosis, is a catabolic process involving the degradation of a cell's own components through the lysosomal machinery. It is a major mechanism by which starving cells reallocate nutrients from unnecessary processes to more-essential processes. Autophagy involves in cell growth, development and homeostasis, helping to maintain a balance between synthesis and degradation. Autophagy resulting in the total demolition of the cell is one of several types of programmed cell death: autophagic cell death (also known as cytoplasmic cell death or type II cell death) [17].

Apoptosis (type I cell death) is another type of programmed cell death in multicellular organisms. As a homeostatic mechanism, apoptosis occurs normally during development and aging to maintain cell populations in tissues. As a defence mechanism, apoptosis also occurs in immune reactions or celluar damages by diseases or noxious agents. Apoptosis leads to morphologically characteristic cell changes including blebbing, loss of cell membrane asymmetry and attachment, cell shrinkage, nuclear fragmentation, chromatin condensation and chromosomal DNA fragmentation [18].

Silibinin's anti-cancer potential has been investigated by numerous researches on multiple cancer cell lines [4–8, 11–13], while we still cannot confirm whether silibinin induces cell death through the same pathways. Our previous researches had shown that silibinin induced protective $O_2^{\cdot-}$ production in MCF-7 cells but displayed cytotoxic effect through a ROS pathway in HT1080 cells, therefore we focused on the ROS/RNS level and how ROS/RNS regulate apoptosis and autophagy in silibinin induced HeLa cell death. In this study, the autophagic and apoptotic effects of silibinin were evaluated in condition of RPMI-1640 medium containing 10% fetal bovine serum (FBS) or without serum. Serum free medium (SFM) could slow cell growth and increased level of cell sensitivity to silibinin-induced autophagy and apoptosis. The use of SFM represents an important tool that allows cell culture to be done with a defined set of conditions as free as possible of confounding variables. Our previous researches had shown that the degree of silymarin's effect on cells changed with the concentration of serum in medium. Cells were much more sensitive to silymarin in medium containing lower concentration of serum [20]. SFM also can mimic a starvation condition to trigger autophagy [13]. Although silibinin is a classic anti-oxidant traditional drug [19], ROS and RNS levels increased in silibinin treated HeLa cells. Therefore, effects of specific antioxidants were also examined in silibinin-treated HeLa cells in relation to cell growth, death and ROS/RNS levels.

Materials and methods

Reagents

Silibinin was obtained from Beijing Institute of Biological Products (Beijing, China); and its purity was determined to be about 99% by HPLC measurement. Silibinin was dissolved in dimethyl sulfoxide (DMSO) to make a stock solution. The concentration of DMSO in all the cell cultures was kept below 0.1% and did not exert any detectable effect on cell growth or death. 3-(4,5-dimetrylthiazol-2-yl)-2,5-diphenyltetrazolium bromide (MTT), acridine orange (AO), propidium iodide (PI), 2',7'-dichlorofluorescein diacetate (H_2DCFDA), 4,5-Diaminofluorescein diacetate (DAF-2DA), monodansylcadervarine (MDC), 3-methyladenine (3-MA), *N*-acetylcysteine (NAC), catalase, superoxide dismutase (SOD), glutathione (GSH), N omega-nitro-l-arginine methyl ester (L-NAME) were purchased from Sigma Chemical (St. Louis, MO, USA). Enhanced chemiluminescent (ECL) substrate kit was purchased from Pierce Biotechnology (Rockford, IL, USA). Polyclonal antibodies against caspase-3 (sc-7148), cytochrome *c* (sc-13561), beclin-1 (sc-10086), LC3 (sc-134226), actin (sc-7210) and horseradish peroxidase-conjugated secondary antibodies were obtained from Santa Cruz Biotechnology (Santa Cruz, CA, USA). MitoTracker® Green FM, MitoTracker® Deep Red 633 and MitoSOX™ Red were obtained from Molecular Probes (Eugene, OR, USA). Lipid Peroxidation MDA Assay Kit was obtained from Beyotime Institute of Biotechnology (Shanghai, PRC).

Cell culture

HeLa cells were obtained from American Type Culture Collection (ATCC, Manassas, VA, USA) and were cultured in RPMI-1640 only or supplemented with 10% fetal bovine serum (FBS) (Dalian Biological

Reagent Factory, Dalian, China), 2 mML-glutamine (Gibco, Grand Island, NY), 100 U/ml penicillin and 100 μg/ml streptomycin at 37°C in 5% CO_2. The cells in the exponential phase of growth were used in experiments.

Cell viability inhibition assay

The inhibitory effect of silibinin on HeLa cell viability was measured by MTT assay. The cells were dispensed in 96-well flat bottom micro titer plates (NUNC, Roskilde, Denmark) at a density of 1.0×10^4 cells per well. After 24 h incubation, they were treated with the tested agents for the indicated time periods. A 20 μl aliquot of MTT solution (5.0 mg/ml) was added to each well followed by 4 h incubation and the optical density was measured using an ELISA reader (Tecan Spectra, Wetzlar, Germany). Each plate contained multiple wells at a given experimental condition and multiple control wells.

The percentage of cell viability inhibition was calculated as follows:

$$\text{Inhibitory ratio } (\%) = (A_{490,\text{control}} - A_{490,\text{sample}})/(A_{490,\text{ control}} - A_{490,\text{ blank}}) \times 100$$

Observation of morphologic changes

The cells were divided into four groups and placed on culture plates for 24 h incubation. Group 1 was cultured in control RPMI-1640 with 10% FBS, group 2 was cultured in RPMI-1640 without FBS, group 3 was treated with silibinin in RPMI-1640 with 10% FBS, and group 4 was treated with silibinin in RPMI-1640 without FBS. The cellular morphology was observed using phase contrast microscopy (Olympus, Tokyo, Japan).

Nuclear damage observed by acridine orange (AO) staining

Cells were labelled with AO (a fluorescent, selective DNA and RNA-binding dye), and then the changes in nuclear morphology of apoptotic cells were examined. After incubation with silibinin for the indicated time periods, the cells were stained with 20 μg/ml AO at 37 °C for 15 min, and then the morphology was observed by a fluorescence microscopy (Olympus, Tokyo, Japan).

Flow cytometric analysis using PI and MDC

HeLa cells were treated with drugs for the indicated time periods, then harvested and rinsed with cold PBS. The cells were fixed in 70% ethanol at 4 °C for at least 18 h. Then the cell pellets were stained with the fluorescent probe solution containing 50 μg/ml PI and 1 mg/ml DNase-free RNaseA in PBS on ice in dark for 1 h. DNA fluorescence of PI-stained cells was evaluated by a FACScan flow cytometry (Becton Dickinson, Franklin Lakes, NJ, USA).

A fluorescent compound, MDC, has been used as a tracer for autophagic vacuoles. HeLa cells were harvested, rinsed with PBS, and then stained with 0.05 mM MDC at 37 °C in dark for 1 h. After incubation, the cells were washed once with PBS. The samples were analyzed by a FACScan flow cytometry.

Lipid peroxidation assay

We used a commercial kit to quantify the generation of malondialdehyde (MDA) according to the manufacturer's protocol. Cells were harvested by trypsinization

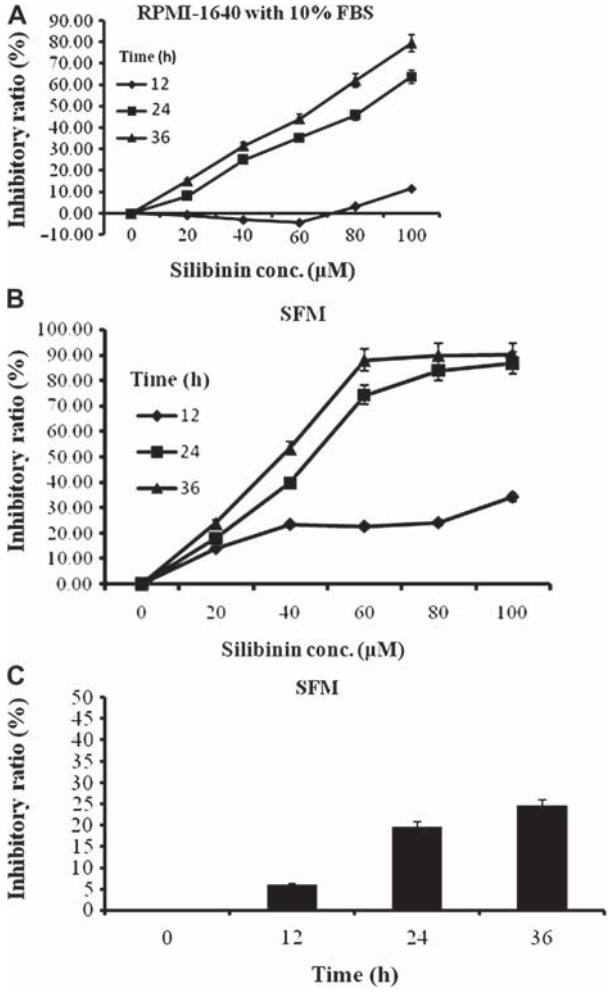

Figure 1. Effect of silibinin on HeLa cell viability. The cells were cultured for 24 h, and then incubated with different concentrations of silibinin (20, 40, 60, 80 and100 μM) for 12, 24 and 36 h. A: The cells were seeded in RPMI-1640 with 10% FBS. B: The cells were cultured without serum. Control: cells incubated in RPMI-1640 without FBS. C: RPMI-1640 withdrawing FBS could inhibit cell viability. The viability was determined by the MTT assay. The data are presented as the mean ± SEM of the results from three independent experiments.

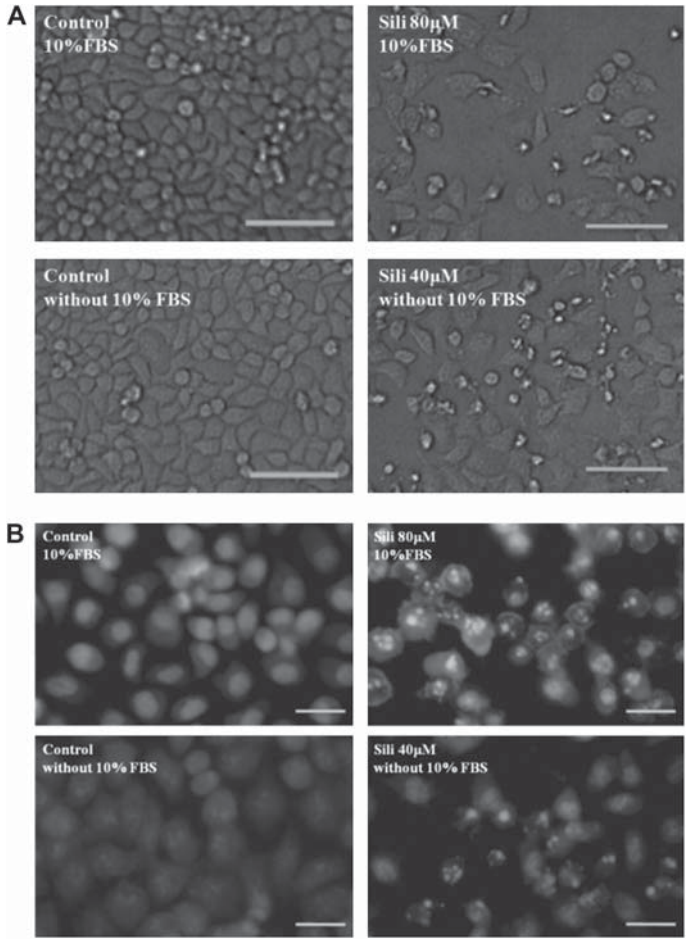

Figure 2. Silibinin induced apoptosis in HeLa cells. A: The cells were observed by contrast microscopy (×100 magnification). B: Changes of nuclear morphology were detected by AO staining (×400 magnification). C: The cells were stained with PI and measured by a flow cytometry after collection. a: The cells were seeded in RPMI-1640 with 10% FBS. b: The cells were cultured without serum. c. The ratio of M1 gated cells were calculated as the subG0/G1 ratio. D: Protein expression of caspase-3 in silibinin-treated HeLa cells at 24 h. a: The cells were seeded in RPMI-1640 with 10% FBS. b: The cells were cultured without serum. E: Release of cytochrome *c* in silibinin-treated HeLa cells at 24 h. a: The cells were seeded in RPMI-1640 with 10% FBS. b: The cells were cultured without serum and were treated with silibinin for 24 h. Cell lysates were separated by 12% SDS-PAGE, and the released protein was detected by Western blot analysis. The data are presented as the mean ± SEM of the results from three independent experiments.

and cellular extracts were prepared by sonication in ice-cold buffer. After sonication, lysed cells were centrifuged at 10,000 × g for 10 min to remove debris. The supernatant was subjected to the measurement of MDA levels. The protein concentration of each sample was determined by a Bio-Rad protein assay reagent (Bio-Rad, Hercules, CA, USA).

Measurement of intracellular ROS and RNS

Intracellular ROS such as H_2O_2, OH and $ONOO^-$ were detected by means of an oxidation-sensitive fluorescent probe dye, 2', 7'-dichlorofluorescein diacetate (H_2DCFDA). H_2DCFDA is a stable non-polar compound that readily diffuses into cells and is hydrolyzed by intracellular esterase to yield H_2DCF, which is trapped within the cells. ROS produced by the cells oxidize H_2DCF to the highly fluorescent compound DCF; thus, the fluorescence intensity is proportional to the amount of ROS produced by the cells [26]. The treated cells were incubated with 10 μM H_2DCFDA in dark at 37 °C for 30 min, then harvested and the pellets were suspended in 1 ml PBS. The samples were analyzed by a FACScan flow cytometry.

Intracellular (RNS) such as NO and $ONOO^-$ were detected by means of an oxidation-sensitive fluorescent probe dye, 4, 5-Diaminofluorescein diacetate (DAF-2DA). DAF-2DA is a non-fluorescent cell permeable reagent that is used to measure free NO and nitric oxide synthase (NOS) activity in living cells under physiological conditions. DAF-2DA enters the cells and its diacetate groups were hydrolyzed by cytosolic esterases, releasing the non-fluorescent DAF-2. DAF-2 then reacts with NO and O_2^- to produce DAF-2T, its triazole fluorescent derivative. The treated cells were incubated with 10 μM DAF-2DA in dark at 37 °C for 30 min, then harvested and the

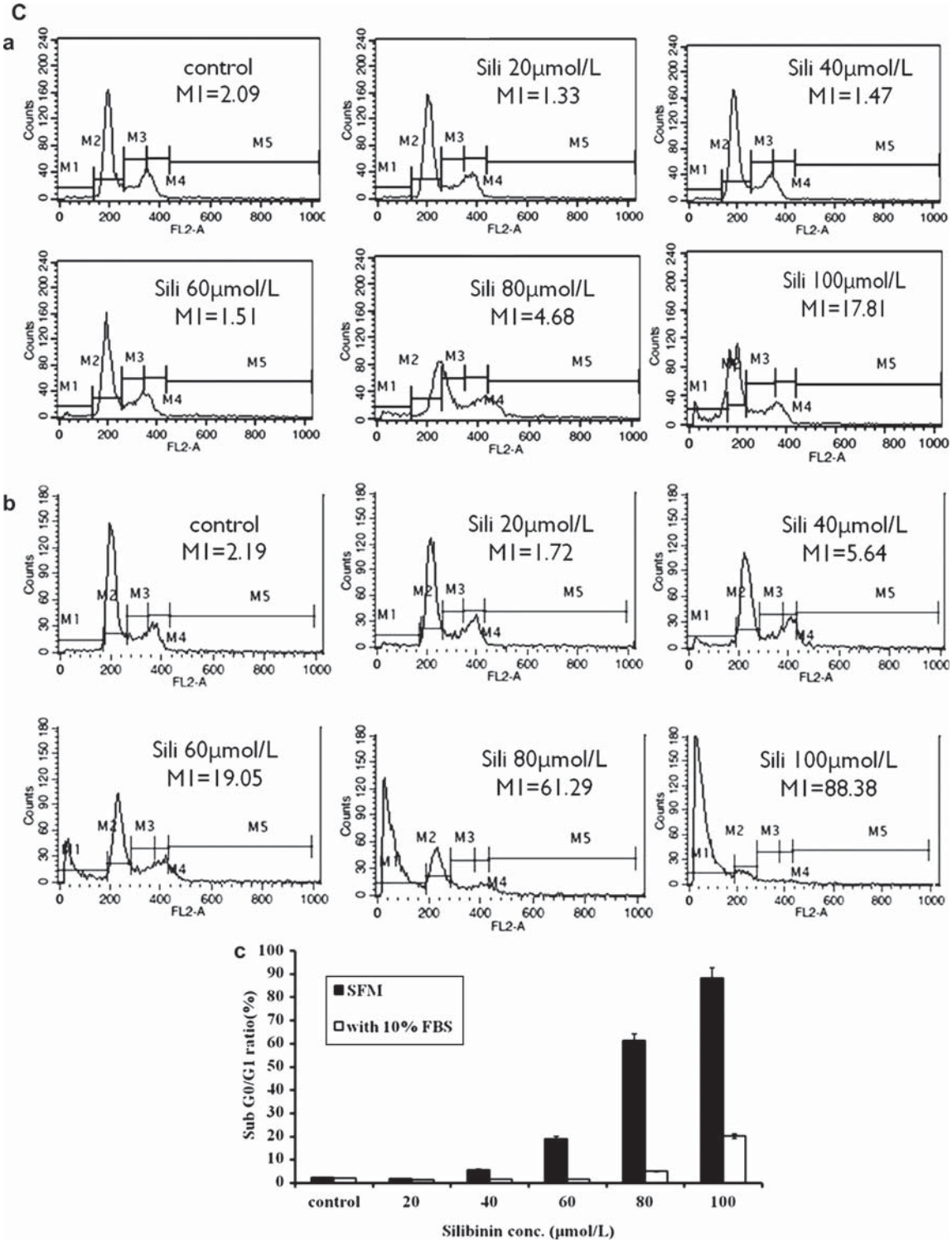

Figure 2. (*Continued*).

pellets were suspended in 1 ml PBS. The samples were analyzed by a FACScan flow cytometry.

Measurement of different types of mitochondria

We used three types of mitochondria-specific labels that distinguish respiring (Mitotracker deep red), total (Mitotracker green) and ROS-generating mitochondria (MitoSOX).

Mitochondria in cells stained with nanomolar concentrations of MitoTracker Green FM dye exhibit bright green, fluorescein-like fluorescence. MitoTracker Deep Red is well suited for multicolor labelling experiments because their red fluorescence is well resolved from the green fluorescence of other probes. MitoTracker Deep Red does not fluoresce until it enters actively respiring cells, where it is oxidized to the corresponding fluorescent mitochondrion-selective probe and then

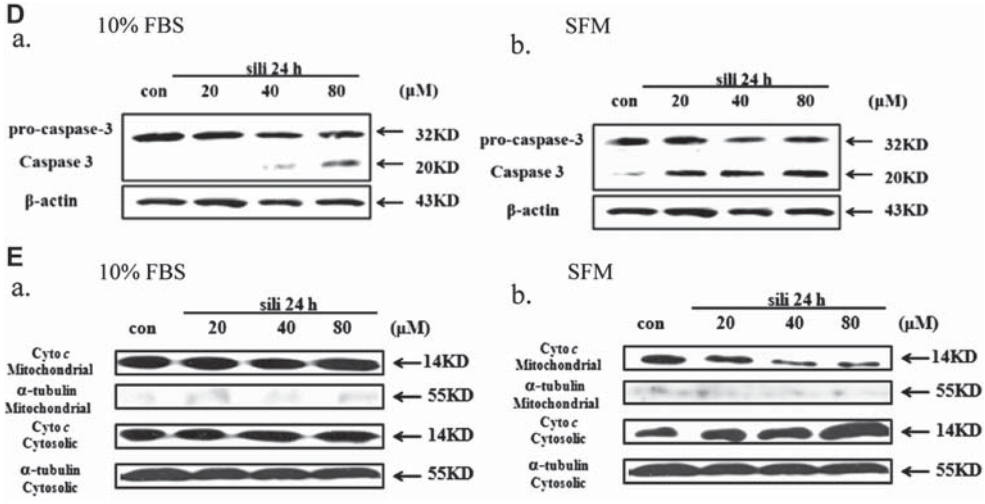

Figure 2. (*Continued*).

sequestered in the mitochondria. The treated cells were co-incubated with 200 nM MitoTracker Green FM and 500 nM MitoTracker Deep Red in the dark at 37 °C for 15 min, then harvested and the pellets were suspended in 1 ml PBS. The samples were analyzed by a FACScan flow cytometry.

MitoSOX™ Red reagent is oxidized by superoxide and exhibits red fluorescence. MitoSOX™ Red reagent is readily oxidized by superoxide but not by other ROS– or RNS–generating systems, and oxidation of the probe is prevented by superoxide dismutase. The oxidation product becomes highly fluorescent upon binding to nucleic acids. The treated cells were co-incubated with 5 μM MitoSOX red in the dark at 37 °C for 15 min, then harvested and the pellets were suspended in 1 ml PBS. The samples were analyzed by a FACScan flow cytometry.

Western blot analysis

Both adherent and floating HeLa cells were harvested, washed twice with ice-cold PBS, and then lysed in whole cell lysis buffer (50 μM 4-(2-hydroxyethyl)-1-piperazineethanesulfonic acid (HEPES), pH 7.4, 1% Triton X-100, 2 mM sodium orthovanadate, 100 mM sodium fluoride, 1 mM Ethylene diamine tetraacetic acid (EDTA), 1 mM Ethylene glycol tetraacetic acid (EGTA) and 1 mM Phenylmethanesulfonylfluoride (PMSF)), supplemented with the proteinase inhibitors, aprotinin 10 μg/ml, leupeptin 10 μg/ml and pepstatin 100 μg/ml at 4 °C for 1 h. After 9,500 × g centrifugation at 4 °C for 15 min, the protein concentration was determined by a Bio-Rad protein assay reagent (Bio-Rad, Hercules, CA, USA). Equal amounts of total proteins were separated by 12% SDS-polyacrylamide gel electrophoresis, and then electroblotted onto nitrocellulose membranes. Proteins were detected with indicated primary antibodies and horseradish peroxidase (HRP)-conjugated secondary antibody and visualized by using ECL substrate kit.

Statistical analysis

All data represented at least three independent experiments and were expressed as mean ± SEM. The data were analyzed by ANOVA using Statistics Package for Social Science software (version 13.0; SPSS, Chicago, IL, USA) and LSD-post-hoc test was employed to assess the statistical significance of difference between control and treated groups. P-values of less than 0.05 were considered statistically significant.

Results

Inhibitory effect of silibinin on HeLa cell viability

The MTT cell-viability assay demonstrated that cell viability was significantly reduced by silibinin in a time- and dose-dependent manner. The IC_{50} for 24 h silibinin treatment was 84.7 μmol/L in media containing 10% FBS and 45.9 μmol/L in SFM, respectively (Figure. 1A, B). When serum was removed, the inhibitory ratio of silibinin-treated HeLa cell viability was increased to two times at 24 h suggesting that serum could protect HeLa cells. This result was confirmed by SFM alone could inhibit HeLa cell viability (Figure 1C).

Silibinin induced apoptosis in HeLa cells cultured with or without 10% FBS

In order to determine the features of silibinin-induced HeLa cell viability reduction, the morphologic changes of the cells were examined. Compared with the control group cultured with or without 10% FBS, significant morphologic changes were observed in cells treated with silibinin for 24 h (Figure 2A). These

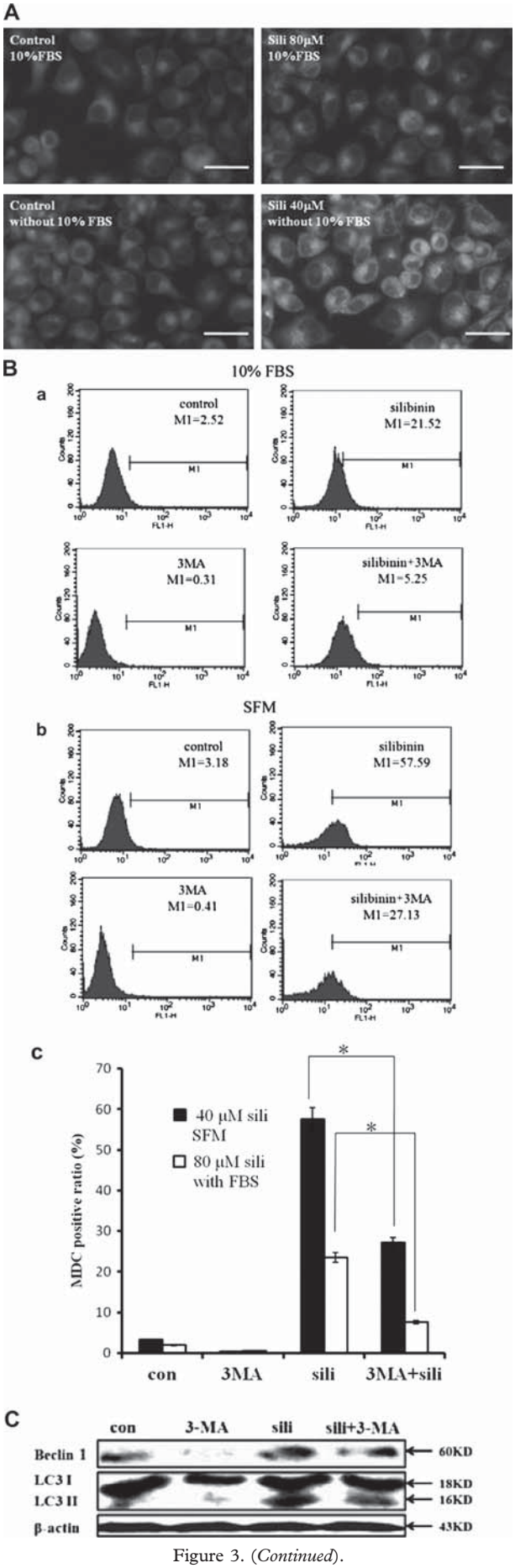

Figure 3. (*Continued*).

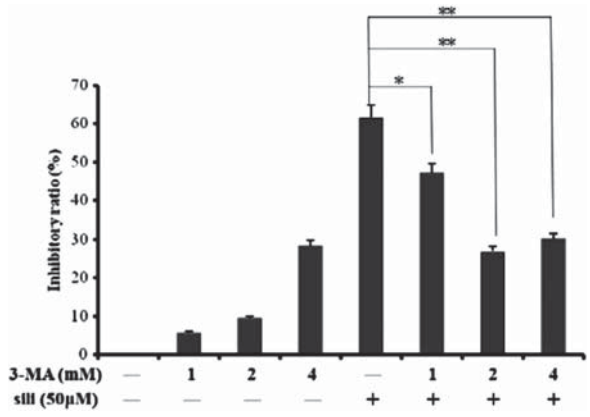

Figure 4. 3-MA inhibited the cytotoxicity of silibinin to HeLa cells. The cells were cultured in SFM for 24 h. The data are presented as the mean ± SEM of the results from three independent experiments. $^{*}P < 0.05$, $^{**}P < 0.01$.

changes were further confirmed by AO staining of cell nuclei. In the control group, the nuclei of the cells were round and homogeneously stained, but silibinin treated cells showed a marked nuclear fragmentation (Figure 2B). PI staining was applied to analyze the changes of cellular DNA contents and silibinin increased the number of cells at subG0/G1 phase in cell cycle in a dose-dependent manner (Figure 2C). When serum was removed, silibinin could induce more significant morphologic changes at a lower dose (Figure 2A and B) and the subG0/G1 ratio of silibinin-treated HeLa cells was increased at 24 h (Figure 2C).

The best recognized biochemical hallmark of both early and late stages of apoptosis is the activation of cysteine proteases (caspases). Detection of active caspase-3 in downstream death pathway is an important method for apoptosis induced by a wide variety of apoptotic signals [21]. It was found that silibinin induced apoptosis by elevated expression of active caspase-3 in HeLa cells either cultured in media containing 10% FBS (Figure 2Da) or SFM (Figure 2Db). In cells undergoing apoptosis, the release of cytochrome *c* from the mitochondria to the cytoplasm has been used as characteristic of apoptosis [22]. Silibinin induced apoptosis by elevated release of cytochrome *c* from the mitochondria to the cytoplasm in the cells either cultured in media containing 10% FBS (Figure 2Ea) or SFM

Figure 3. Silibinin induced autophagy in HeLa cells. A: Cellular fluorescent density was examined in the absence or presence of silibinin at 12 h (×400 magnification); the cells were labelled with MDC. B: Quantitative analysis detected a positive ratio of MDC staining by flow cytometry. The cells were treated with silibinin (40 or 80 μM) and/or 3-MA (2 mM), and harvested after 12 h. a: The cells were seeded in RPMI-1640 with 10% FBS. b: The cells were cultured without serum. c: The ratio of M1 gated cells were calculated as the MDC positive ratio. C: Protein expression of beclin-1 and LC3 in silibinin-treated HeLa cells cultured in SFM at 12 h. Cell lysates were separated by 12% SDS-PAGE, and the protein expression were detected by Western blot analysis. The data are presented as the mean ± SEM of the results from three independent experiments. $^{*}P < 0.05$.

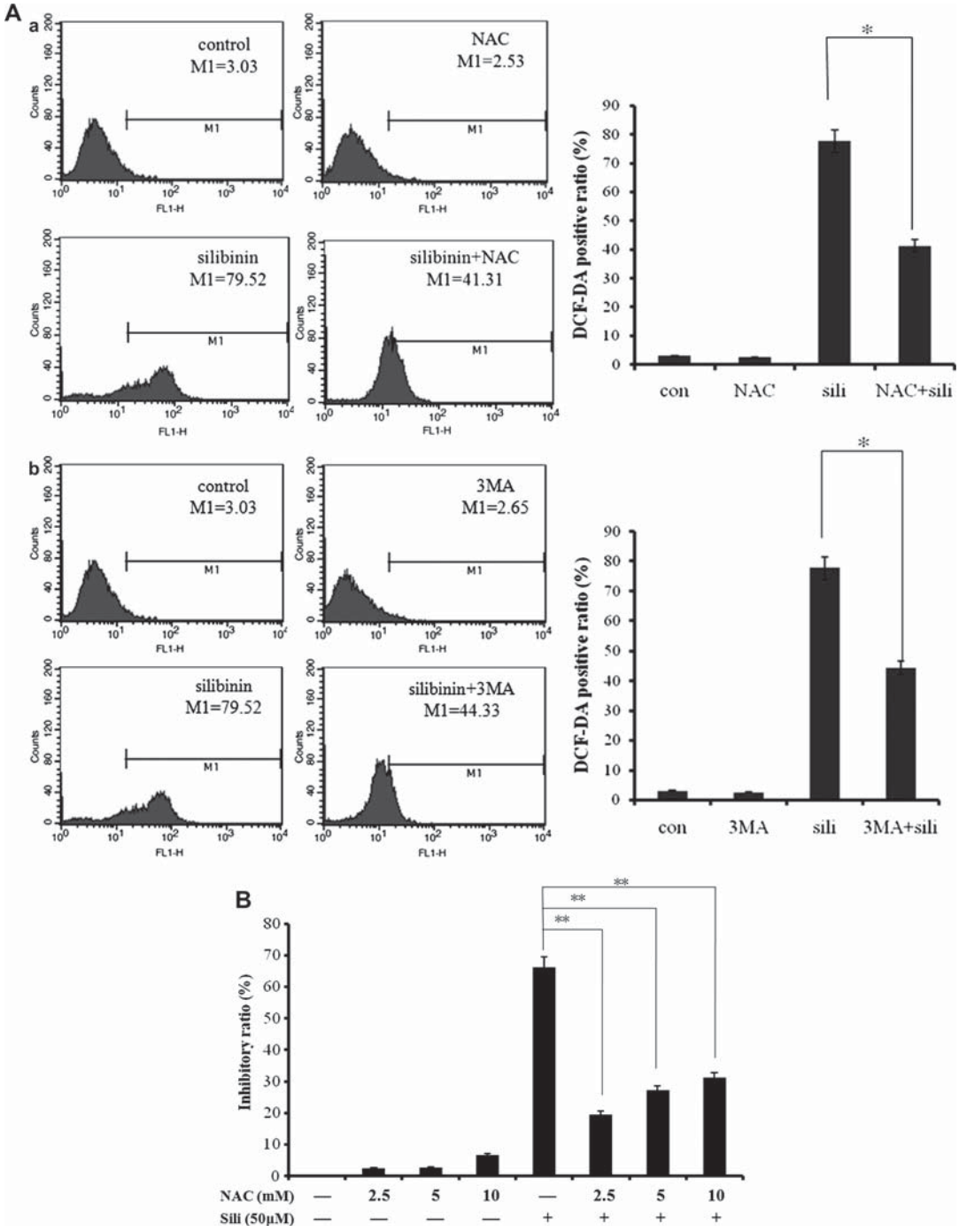

Figure 5. Silibinin induced apoptosis and autophagy by ROS production in HeLa cells. A: ROS level was detected by a flow cytometry staining with DCF-DA. a: The cells were incubated with silibinin (50 μM) or co-incubated with NAC (2.5 mM) for 12 h. b: The cells were incubated with silibinin (50 μM) or co-incubated with 3-MA for 12h. The ratio of M1 gated cells were calculated as the DCF-DA positive ratio. B: The cells were incubated with silibinin or co-incubated with NAC for 24 h, and the inhibitory ratio was measured by MTT assay. C: a: The MDC fluorescent intensity of treated cells was analyzed by a flow cytometry. The ratio of M1 gated cells were calculated as the MDC positive ratio. b: The cells were stained with PI and measured by a flow cytometry after collection. The ratio of M1 gated cells were calculated as the subG0/G1 ratio. The data are presented as the mean ± SEM of the results from three independent experiments. $*P < 0.05$, $**P < 0.01$.

(Figure 2Eb). The silibinin-induced capase-3 protein activation and cytochrome *c* release increased in HeLa cells cultured in SFM compared to the cells cultured in media containing 10% FBS (Figure 2D, E). These results suggested that silibinin could induce apoptotic cell death in HeLa cells.

Silibinin induced autophagy in HeLa cells cultured with or without 10% FBS

In our previous researches, silibinin induced autophagy in multiple cell lines; therefore, we examined autophagy in silibinin treated HeLa cells. Auto-fluorescent

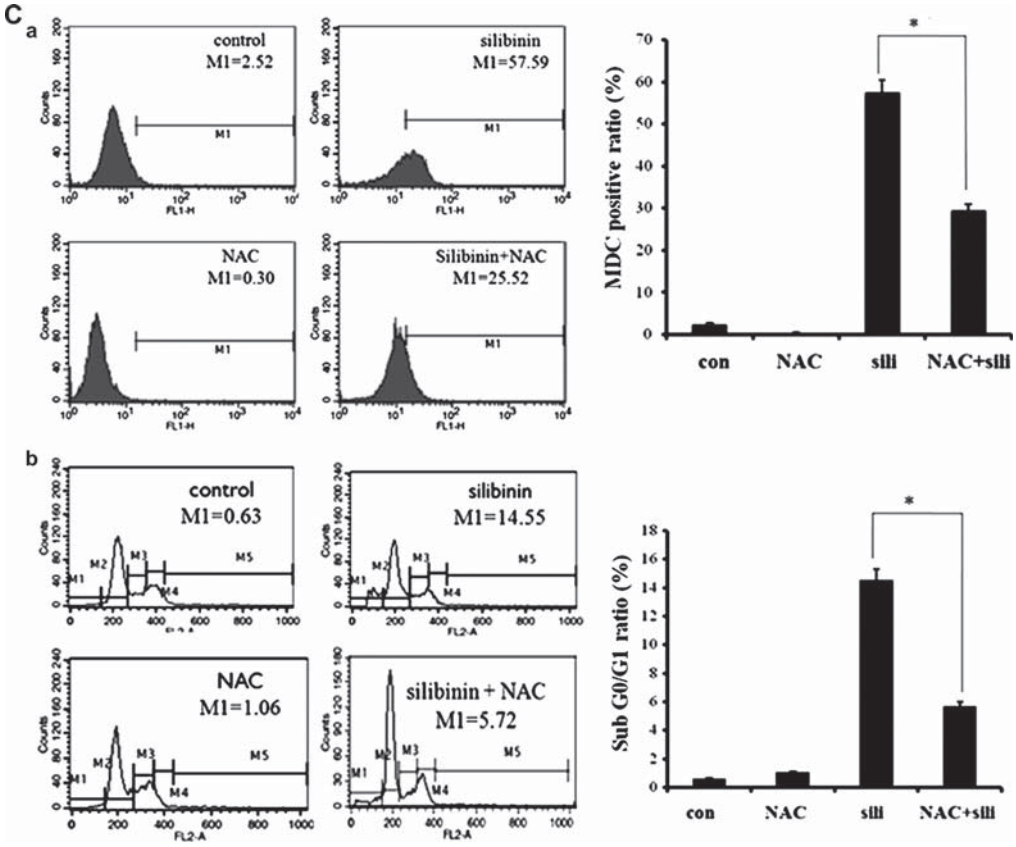

Figure 5. (*Continued*).

compound MDC was used for *in vivo* labelling of autophagic vacuoles [23]. Compared with the control group, the silibinin-treated group showed higher fluorescent intensity and more MDC labelled particles were detected at 12 h (Figure 3A), representing that silibinin increased MDC recruitment to autophagosomes in the cytoplasm of the cells. Subsequently, the flow cytometric analysis also showed that the percentage of MDC-positive cells treated by silibinin was increased compared to those in the control group. Autophagy was more significant in the silibinin (40 μM) treated cells cultured in SFM for 12 h than those treated by higher dose (80 μM) of silibinin in RPMI-1640 containing 10% FBS. The specific autophagic inhibitor 3-MA [24] decreased the number of MDC-positive cells (Figure 3B).

Beclin 1, the mammalian orthologue of yeast Atg6, is part of the class III phosphatidylinositol 3-kinase (PI3K) complex that induces autophagy [25]. Microtubule-associated protein light chain 3 (LC3) is now widely used to monitor autophagy. Endogenous LC3 is detected as two bands in SDS-PAGE and immunoblotting: LC3-I, which is cytosolic, and the other LC3-II, which exists on cytoplasmic membranes and autophagosomes, and much less on autolysosomes. The amount of LC3-II is related to the number of autophagosomes, serving as a good indicator of autophagosome formation [27]. Silibinin induced much more significant autophagy in cells cultured in SFM, therefore we focused on protein expression of beclin 1 and LC3-II in cells cultured in SFM. Protein expression of beclin 1 and LC3-II were up-regulated in silibinin-treated cells cultured in SFM at 12 h, and 3-MA reversed this effect of silibinin (Figure 3C).

Since the cells cultured in SFM were much more sensitive to silibinin, our following experiments were focused on cells cultured in SFM, and all data shown were the effects of silibinin on the HeLa cells in the serum free culture.

Inhibition of autophagy elevated survival of silibinin-treated HeLa cells

Autophagy is a process for turnover of intracellular organelles and molecules that protects cells during stress responses. At the same time, extensive autophagy is commonly observed in dying cells, leading to its classification as an alternative form of programmed cell death [28]. Cell death is also triggered by autophagic degradation of apoptosis inhibitors [29]. MTT assay indicated that 3-MA decreased the inhibitory effect of silibinin on HeLa cell viability in serum free culture (Figure 4). High dose (4 mM) of 3-MA exhibited inhibition to cell viability, and 2 mM of 3-MA showed the maximum protection to cells. Silibinin-induced autophagy led HeLa cells to death, instead of survival (Figure 4).

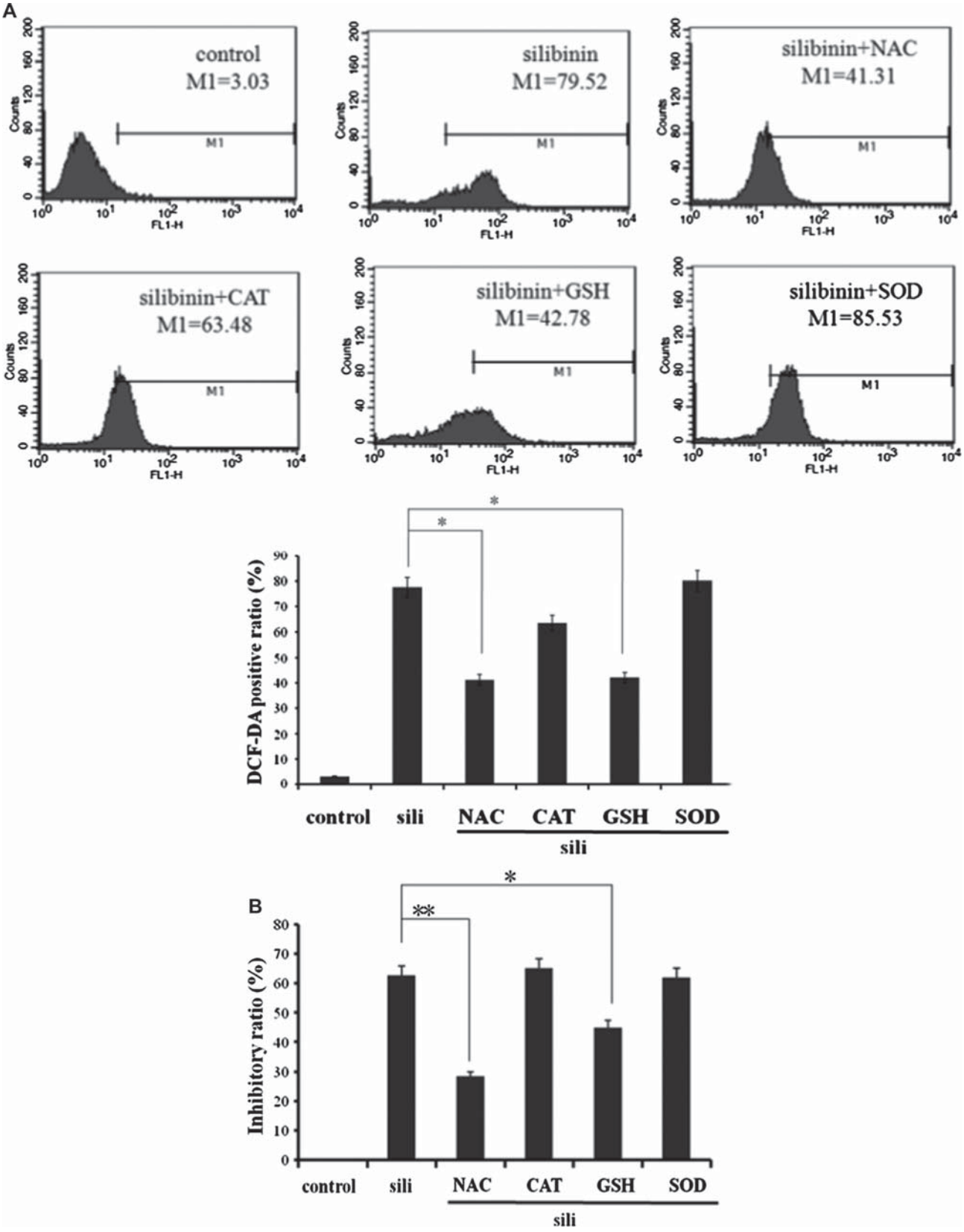

Figure 6. OH was the major ROS that participated in silibinin-induced cell death. The cells were incubated with silibinin (50 μM) or co-incubated with specific ROS scavengers. NAC (2.5 mM), GSH (2.5 mM), CAT (100 U/ml), SOD (100 U/ml). A: ROS level was detected by a flow cytometry stained with DCF-DA. The ratio of M1 gated cells were calculated as the DCF-DA ratio. B: The inhibitory ratio was measured by MTT assay. C: The positive ratio of MDC staining was analyzed by a flow cytometry. The ratio of M1 gated cells were calculated as the MDC ratio. D: The cells were stained with PI and measured by a flow cytometry after collection. The ratio of M1 gated cells were calculated as the subG0/G1 ratio. The data are presented as the mean ± SEM of the results from three independent experiments. $*P < 0.05$; $**P < 0.01$.

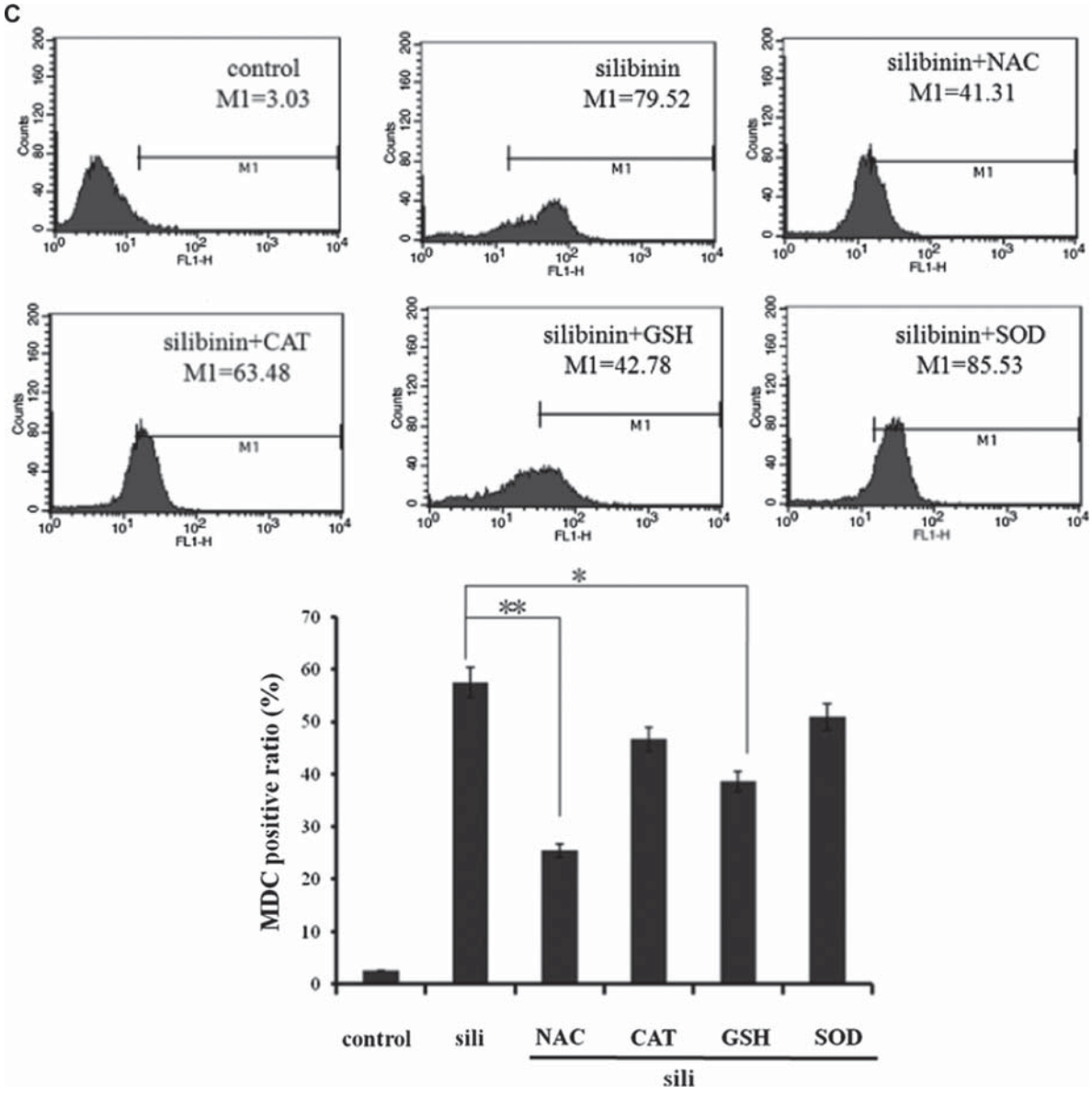

Figure 6. (*Continued*).

Silibinin induced apoptosis and autophagy by ROS increase in HeLa cells

Though silibinin is a classic anti-oxidant drug, ROS level was increased in silibinin treated HeLa cells in serum free culture. NAC, a ROS scavenger, markedly decreased the level of ROS in silibinin treated HeLa cells (Figure 5Aa). 3-MA also inhibited generation of ROS (Figure 5Ab), indicating that inhibition of autophagy reduced ROS in the cells. NAC decreased the inhibitory effect of silibinin on HeLa cell viability in serum free culture, but high dose (10 mM) of NAC exhibited inhibition to the cell viability (Figure 5B). To investigate whether the protection of NAC was attributed to autophagy or apoptosis, MDC and PI staining were applied, and NAC treatment lowered MDC positive ratio (Figure 5Ca), furthermore, NAC reduced the number of cells at subG0/G1 phase (Figure 5Cb). Autophagic and apoptotic cell death is related to ROS increase, and ROS scavenger NAC could rescue the cells by reversing both apoptosis and autophagy in silibinin-treated HeLa cells.

Hydroxyl radical (·OH) was the major ROS induced by silibinin

Forms of ROS in silibinin-treated cells in serum free culture were determined by exogenous enzyme antioxidants (SOD, catalase) or non-enzyme antioxidants (NAC, GSH). The generation of ROS was evaluated by DCF-DA staining. OH scavenger GSH-treatment reduced ROS level significantly. Catalase treatment slightly reduced ROS level and SOD had no effect on ROS level (Figure 6A). It has been reported that catalase is used by cells to rapidly catalyze the decomposition of hydrogen peroxide (H_2O_2) into less reactive gaseous oxygen and water molecules [30], and SOD specifically catalyzes the reduction of superoxide anions (O_2^-) [31].

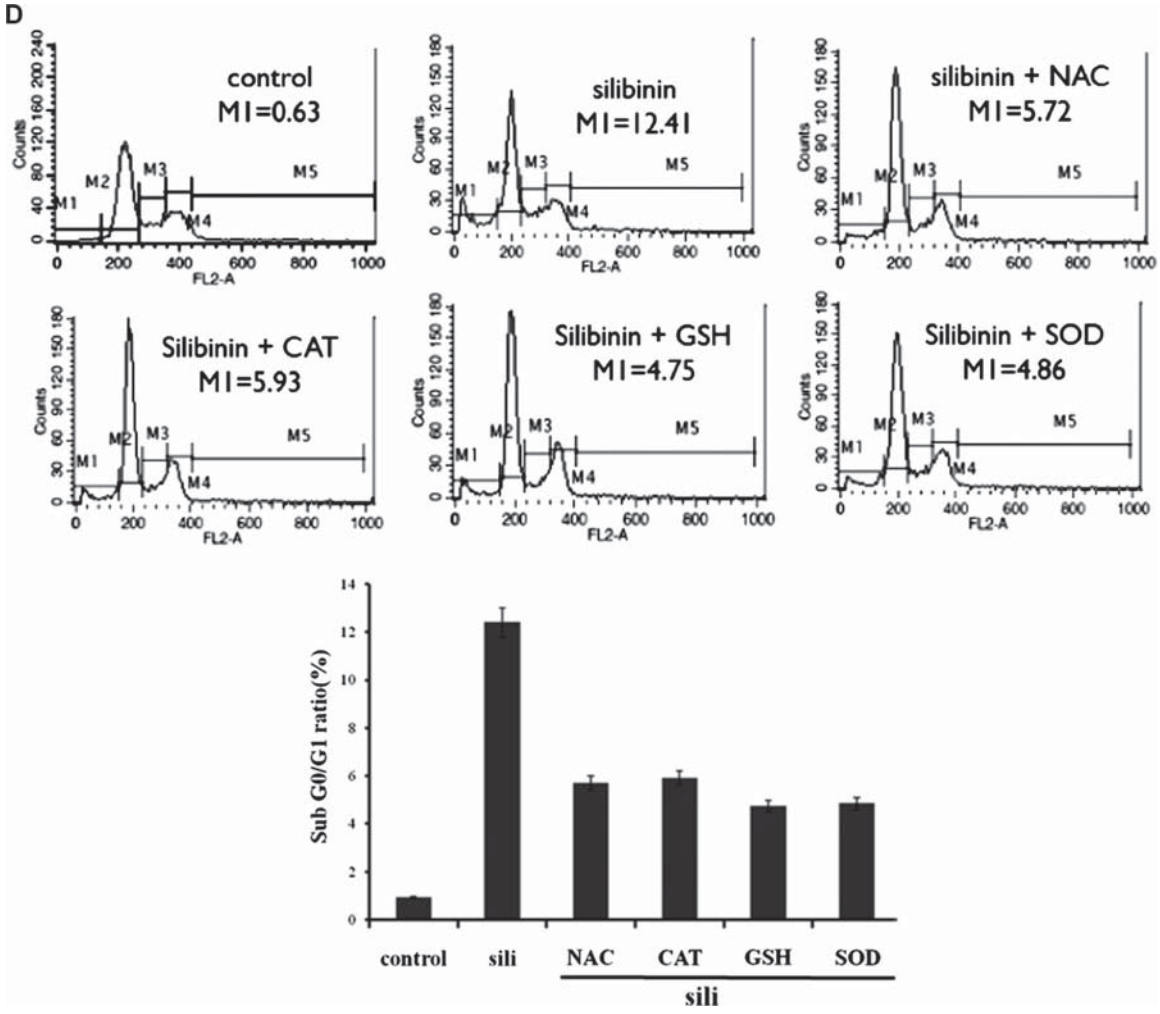

Figure 6. (*Continued*).

Hydroxyl radical is the major form of intracellular ROS generated by silibinin in HeLa cells. Contribution of antioxidants to viability of silibinin-treated cells was measured by MTT assay. GSH reversed the inhibitory effect of silibinin on HeLa cell viability in serum free culture, while catalase and SOD had no such effect (Figure 6B). Autophagy of cells in media with different antioxidants plus silibinin was examined by MDC staining. GSH significantly decreased MDC positive ratio (Figure 6C), indicating that silibinin-induced autophagy in the cells was also mainly mediated by OH. Apoptosis of cells in media with different antioxidants plus silibinin was examined by PI staining. Results showed that all types of ROS scavenger decreased the number of cells at subG0/G1 phase (Figure 6D). It was concluded that GSH decreased ROS level and protected the cells. Silibinin-induced hydroxyl radical inhibited cell viability mainly through autophagy, but not apoptosis.

Silibinin induced apoptosis and autophagy by RNS increase in HeLa cells

RNS level was increased in silibinin treated HeLa cells as well as ROS level. Silibinin increased RNS level in a dose-dependent manner (Figure 7Aa). Overexpression of NOS resulted in cytotoxic concentrations of NO and RNS which led to cell death. High dose of L-NAME was used as NOS inhibitor, and decreased the RNS level (Figure 7Ab). MTT assay was used to examine the protective effect of L-NAME on cells treated by silibinin. High dose of L-NAME decreased the inhibitory effect of silibinin in serum free culture (Figure 7 B). To investigate whether the protection by L-NAME was attributed to apoptosis or autophagy, PI and MDC staining were applied. L-NAME treatment reduced the number of cells at subG0/G1 phase (Figure 7Ca). Furthermore, L-NAME lowered MDC positive ratio (Figure 7Cb). Both ROS scavengers and 3-MA could decrease RNS level in silibinin-treated HeLa cells (Figure 7D), suggesting that RNS level was associated with ROS level in silibinin-treated HeLa cells.

Silibinin triggered the cell damage by interruption of the respiring function of mitochondria

One of the important aspects of damage caused by ROS is the oxidation of lipids. To determine if

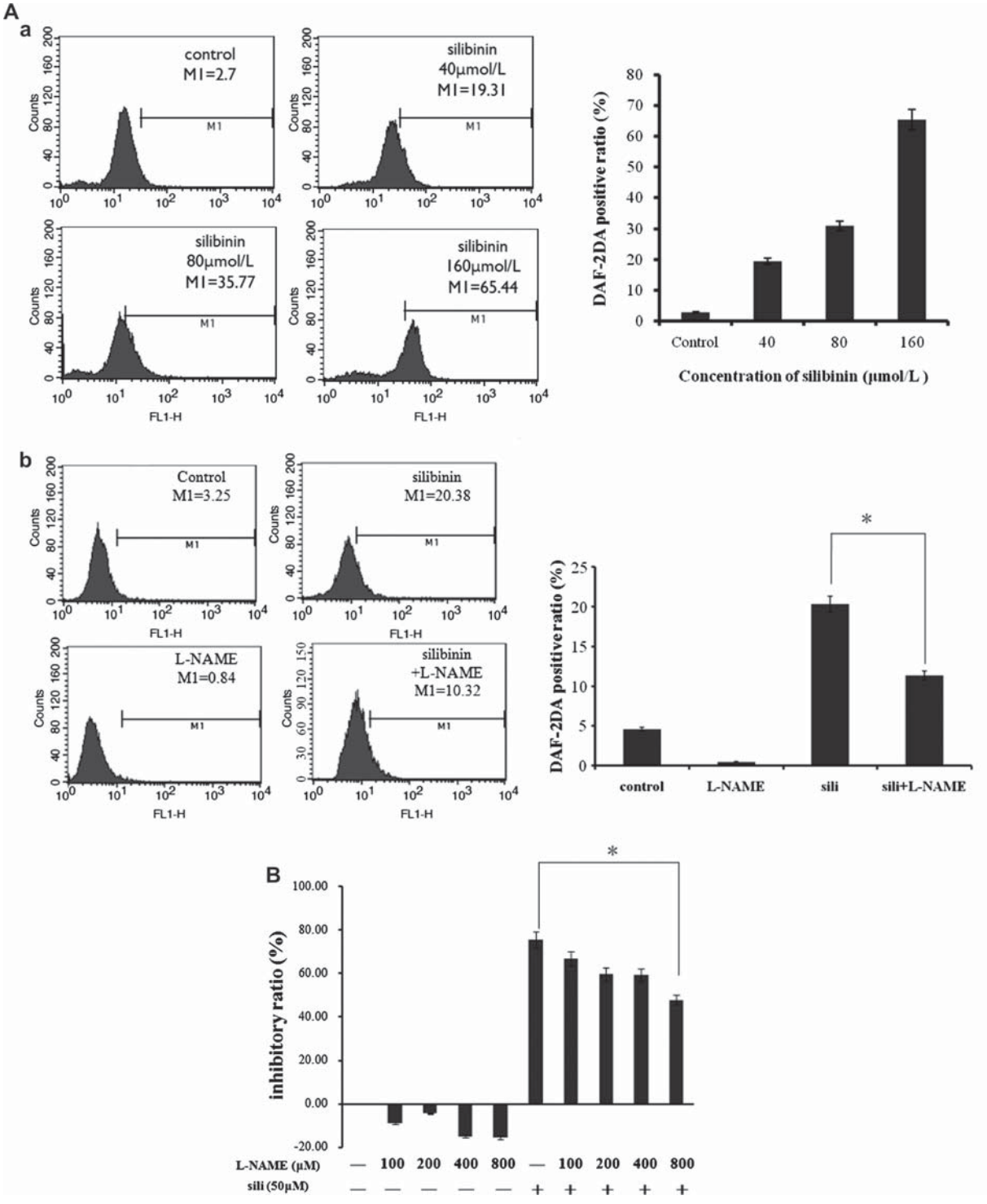

Figure 7. Silibinin induced apoptosis and autophagy through RNS in HeLa cells. A: RNS level was detected by a flow cytometry staining with DAF-2DA. a: The cells were incubated with different concentrations of silibinin for 12 h. b: The cells were incubated with silibinin(50 μM) or co-incubated with L-NAME (800 μM) for 12 h. The ratio of M1 gated cells were calculated as the DAF-2DA ratio. B: The cells were incubated with silibinin or co-incubated with different concentrations of L-NAME for 24 h, and the inhibitory ratio was measured by MTT assay. C: a: The cells were incubated with silibinin or co-incubated with L-NAME (800 μM) for 24 h. Then cells were stained with PI and measured by a flow cytometry after collection. The ratio of M1 gated cells were calculated as the subG0/G1 ratio. b: The cells were incubated with silibinin or co-incubated with L-NAME (800 μM) for 12 h. Then MDC fluorescent intensity of treated cells was analyzed by a flow cytometry. The ratio of M1 gated cells were calculated as the MDC ratio. D: The cells were incubated with silibinin or co-incubated with specific ROS scavengers and 3-MA, and the RNS level was detected by a flow cytometry. The ratio of M1 gated cells were calculated as the DAF-2DA ratio. The data are presented as the mean ± SEM of the results from three independent experiments. $*P < 0.05$.

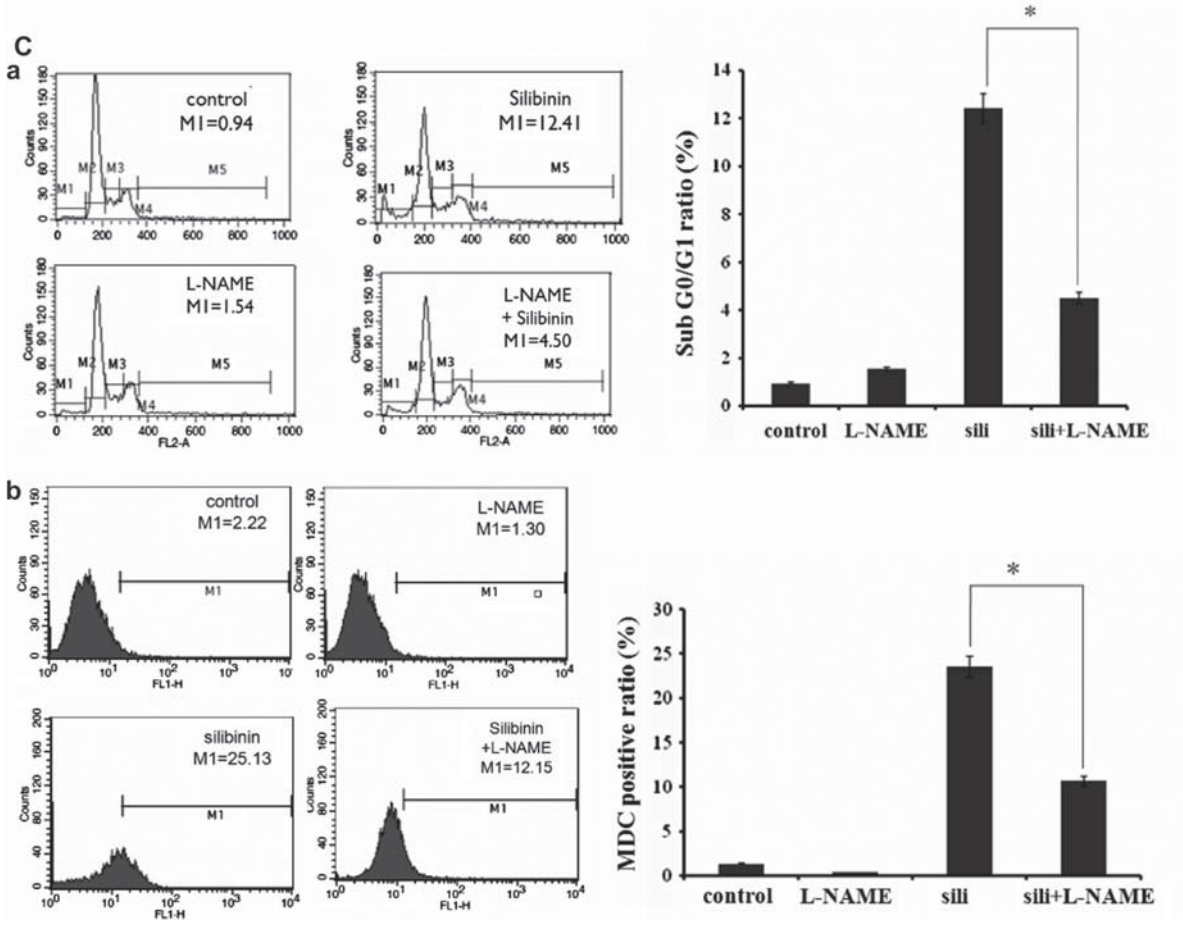

Figure 7. (*Continued*).

silibinin can trigger this damage, we measured the lipid peroxidation in HeLa cells treated with different concentrations of silibinin. We found that MDA generation was increased to1.7 fold by 50 μM silibinin and to 4 fold by 100 μM silibinin (Figure 8A), indicating that silibinin up-regulated the ROS level in HeLa cell and triggered the oxidative damage. In one of our colleagues' research, observation showed that silibinin might affect the mitochondrial respiratory chain to up-regulated the ROS level [11]. To investigate whether silibinin caused the oxidative damage by interrupting the respiratory chain, we used three types of mitochondria-specific dye which distinguish respiring (Mitotracker deep red), total (Mitotracker green) and ROS-generating mitochondria (MitoSOX). Respiratory chain complex I and complex III were the sites where electrons leak to oxygen and result in superoxide production [46]. In agreement with previous reports [47], administration of the complex I inhibitor rotenone and complex III inhibitor antimycin A resulted in robust ROS production (Figure 8B). Silibinin (50 μM) increased the ratio of respiration-interrupted mitochondria but did not obviously affect the ratio of superoxide -generating mitochondria (Figure 8Ba and b). Since MitoSOX is readily oxidized by superoxide but not by other ROS or RNS, silibinin might not affect the production of superoxide anions in mitochondria (Figure 8Ba). This result is in agreement with aforementioned results that superoxide anions were not the major ROS induced by silibinin. Silibinin could interrupt the respiring function of mitochondria, leading ROS production and resultant oxidative damage.

Discussion

Silibinin was reported to have anticancer and antioxidant properties. Our previous studies showed that silibinin exhibited dual effects on multiple cell lines. Silibinin prevented UV-induced HaCaT cell apoptosis partially through inhibition of caspase-8 pathway [32], while silibinin induced autophagic and apoptotic cell death in HT1080 cells [13]. Silibinin enhanced HT1080 cell growth at low dose and short-time culture, while silibinin inhibited cell growth at higher doses and longer-time culture in the cells [13]. In this study, silibinin suppressed HeLa cell growth. These results indicated that the function of silibinin was switched by different signals in multiple cell lines. More significant inhibitory ratio was observed under the nutrient deprivation condition mimicked by serum-withdrawal in HeLa cells, similar to in HT1080 cells. This result suggested that silibinin induced more obvious cell growth suppression in aggravated environment.

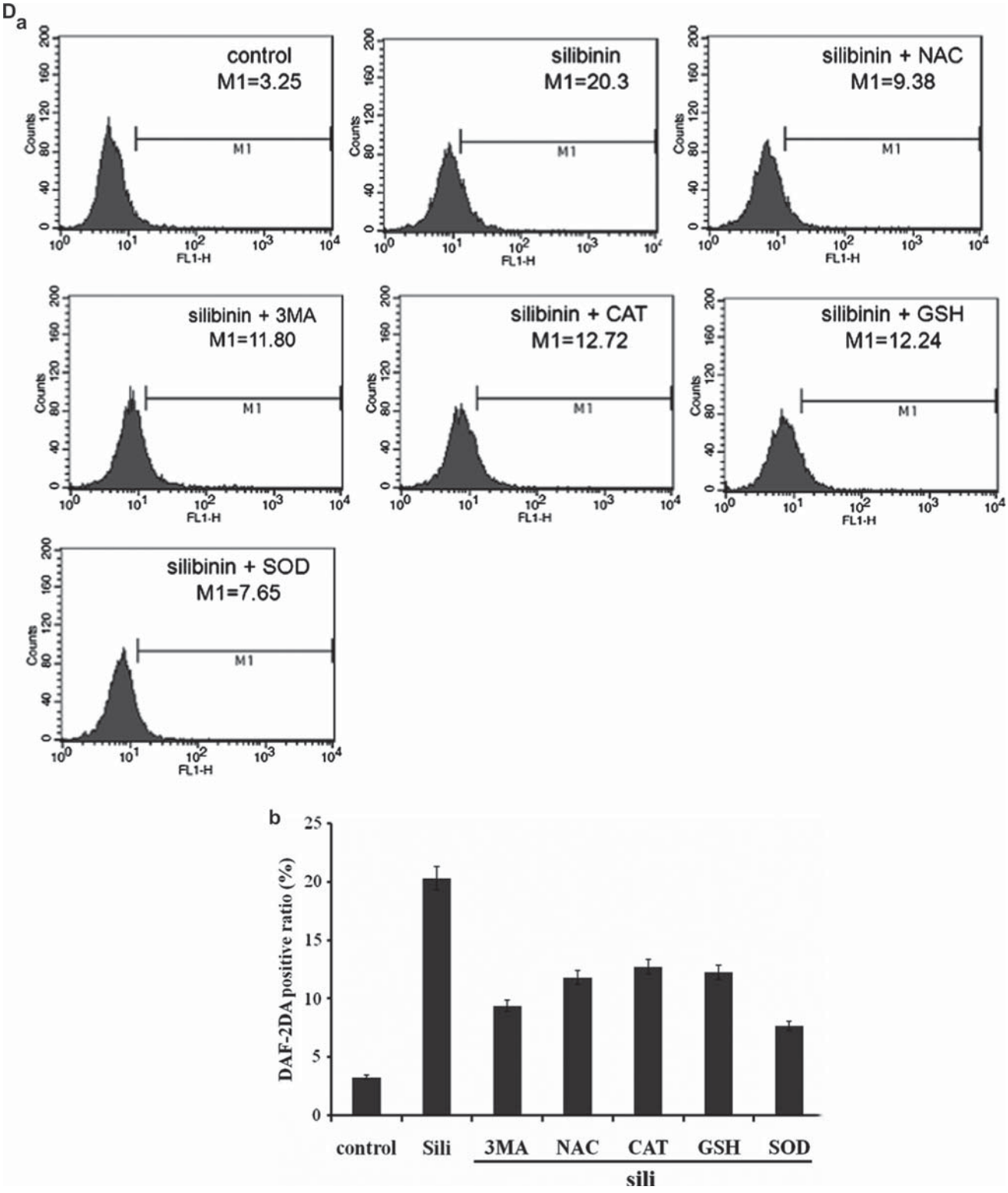

Figure 7. (*Continued*).

Silibinin could induce apoptosis and autophagy in HeLa cells; however the functional relationship between autophagy and apoptosis is complex. Autophagy not only provides a survival advantage to the cells undergoing nutrient deprivation or other stresses but also links to the actual death process itself. Both autophagy and apoptosis lead to cell death, and they act as partners. They may act independently in similar pathways, or one may be influenced by another. Autophagy has been shown to be necessary for apoptotic cell death, placing it upstream of apoptosis, whereas modulating an independent means of death [33]. After inhibition of autophagy with 3-MA, inhibitory ratio declined, suggesting that autophagy induced by silibinin might enhance HeLa cell death.

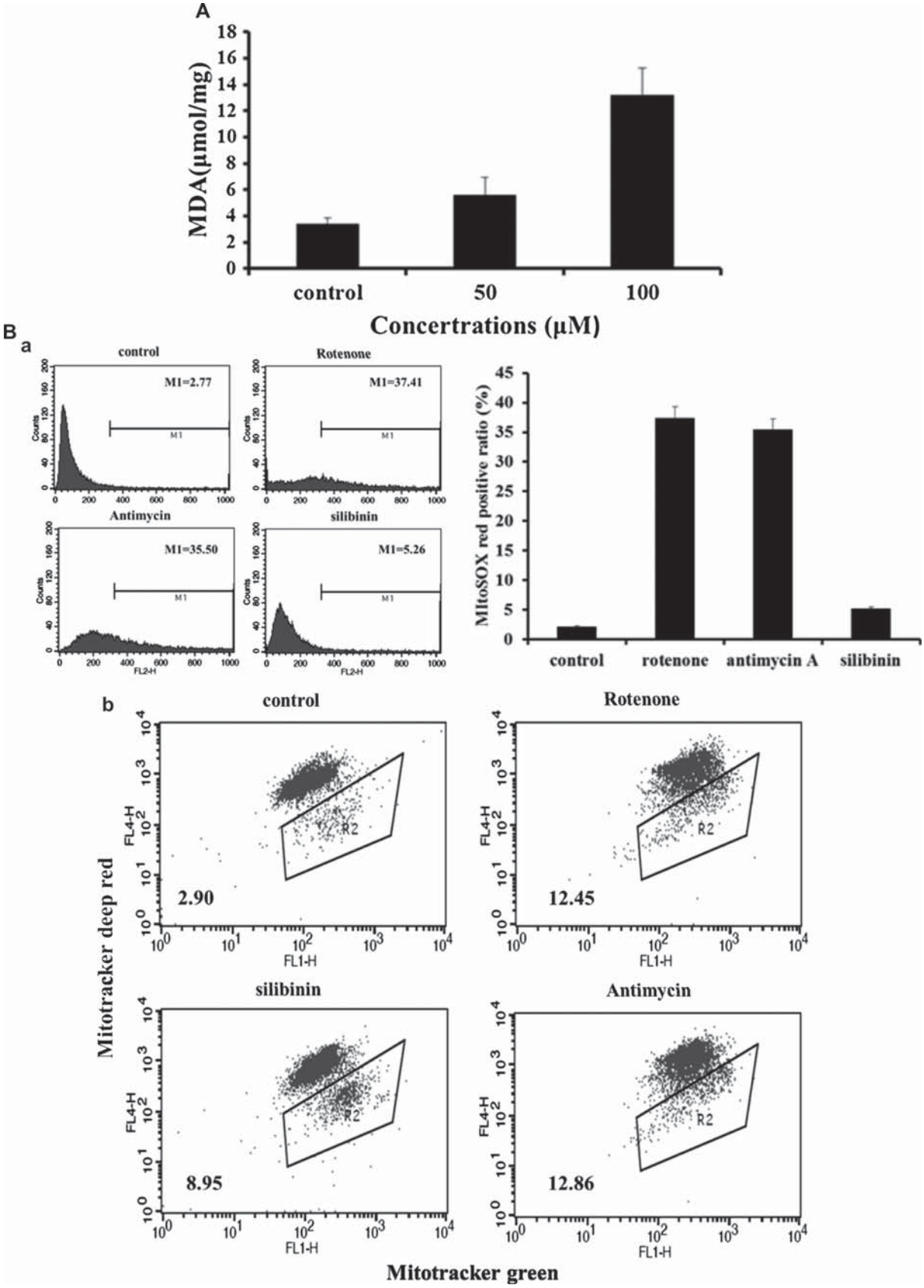

Figure 8. Silibinin triggered the cell damage and interrupted the respiring function of mitochondria. A: Analysis of MDA generation in silibinin treated HeLa cells. B: The cells were incubated with silibinin (50 μM), rotenone (10 μM) and antimycin A (1 μM). a: ROS-generating mitochondria ratio was detected by a flow cytometry stained with MitoSOX red. b: Respiring mitochondria ratio was detected by a flow cytometry stained with Mitotracker green FM and Mitotracker deep red. The data are presented as the mean ± SEM of the results from three independent experiments.

At the molecular level, the cross-talk between apoptosis and autophagy is manifested by the numerous genes that are shared by both pathways. These pathways include mTOR [34], PI3K/Akt signal [34], MAPK/ERK1/2 [35] and mitochondrial pathways [36]. Mitochondria are important regulators of both apoptosis and autophagy and are both source and target of ROS. It was reported that ROS mediated mitochondrially-induced autophagic [37] and apoptotic cell death [38]. RNS is another type of free radicals linked to ROS. RNS and ROS can induce apoptosis by common pathways [39]. Recently, several studies have demonstrated that RNS may be also involved in induction of autophagy [40, 41].

ROS are molecules or ions that are formed by the incomplete one-electron reduction of oxygen, O_2^-, H_2O_2,·OH and others. It was reported that silibinin was able to scavenge oxygen free radicals, including O_2^-, H_2O_2 and OH [42]. The activity of both superoxide dismutase and glutathione peroxidase could be increased by silibinin in human red blood cells [43]. But silibinin was also found to inhibit cell proliferation by increasing ROS level in glioma [44] and HT1080 cells [13]. The mechanisms of silibinin's dual effects are still not clear.

Our results showed that silibinin induced ROS generation in HeLa cells, which was down-regulated by a ROS scavenger NAC. MDC positive ratio and subG0/G1 ratio were also down-regulated by NAC. NAC reversed both autophagy and apoptosis induced by silibinin, indicating that NAC could affect both pathways to exert its protective effect. 3-MA, as well as NAC, decreased ROS level in silibinin treated HeLa cells. It was reported that autophagy pathways contributed to cell resistance against ROS damage [45] and our results also suggested that a positive feedback existed between autophagy and ROS. In this study, OH scavenger GSH reduced ROS induced by silibinin, but H_2O_2 scavenger catalase and O_2^- scavenger SOD had no such effect. Silibinin induced RNS generation in HeLa, which was down-regulated by a NOS inhibitor L-NAME. L-NAME also reduced ROS induced by silibinin and reversed both autophagy and apoptosis. ROS scavengers also reduced RNS induced by silibinin. SubG0/G1 ratio of silibinin treated cells was lower than MDC positive ratio. ROS scavengers reduced subG0/G1 ratio but failed to reduce inhibitory ratio.

According to these, silibinin triggered generation of ROS, and silibinin itself could not scavenge these ROS. Silibinin was not a ROS scavenger but an inducer. Silibinin also triggered generation of RNS, and induced-ROS affected this pathway. Silibinin's growth inhibitory effect might mainly contribute to the induction of ROS/RNS-mediated autophagy.

Declaration of interest

The authors report no conflicts of interest. The authors alone are responsible for the content and writing of the paper. This research was funded by the National Key Scientific Project for New Drug Discovery and Development (2009ZX09301-012), P.R.China.

References

[1] Dehmlow C, Erhard J, de Groot H. Inhibition of Kupffer cell functions as an explanation for the hepatoprotective properties of silibinin. Hepatology 1996;23(4):749–754.

[2] Haddad Y, Vallerand D, Brault A, Haddad PS. Antioxidant and hepatoprotective effects of silibinin in a rat model of non-alcoholic steatohepatitis. Evid Based Complement Alternat Med. 2009 Nov 1. Available:http://ecam.oxfordjournals.org/cgi/reprint/nep164v1.pdf via the INTERNET.

[3] Al-Anati L, Essid E, Reinehr R, Petzinger E. Silibinin protects OTA-mediated TNF-alpha release from perfused rat livers and isolated rat Kupffer cells. Mol Nutr Food Res 2009; 53(4):460–466.

[4] Mokhtari MJ, Motamed N, Shokrgozar MA. Evaluation of silibinin on the viability, migration and adhesion of the human prostate adenocarcinoma (PC-3) cell line. Cell Biol Int 2008;32(8):888–892.

[5] Tyagi AK, Agarwal C, Chan DC, Agarwal R. Synergistic anticancer effects of silibinin with conventional cytotoxic agents doxorubicin, cisplatin and carboplatin against human breast carcinoma MCF-7 and MDA-MB468 cells. Oncol Rep 2004;11(2):493–499.

[6] Bhatia N, Zhao J, Wolf DM, Agarwal R. Inhibition of human carcinoma cell growth and DNA synthesis by silibinin, an active constituent of milk thistle: comparison with silymarin. Cancer Lett 1999;147(1–2):77–84.

[7] Hogan FS, Krishnegowda NK, Mikhailova M, Kahlenberg MS. Flavonoid, silibinin, inhibits proliferation and promotes cell-cycle arrest of human colon cancer. J Surg Res 2007; 143(1):58–65.

[8] Sharma G, Singh RP, Chan DC, Agarwal R. Silibinin induces growth inhibition and apoptotic cell death in human lung carcinoma cells. Anticancer Res (2003);23(3B): 2649–2655.

[9] Zhou B, Wu LJ, Tashiro S, Onodera S, Uchiumi F, Ikejima T. Silibinin protects rat cardiac myocyte from isoproterenol-induced DNA damage independent on regulation of cell cycle. Biol Pharm Bull 2006;29(9):1900–1905.

[10] Zhou B, Wu LJ, Tashiro S, Onodera S, Uchiumi F, Ikejima T. Protective effect of silibinin against isoproterenol-induced injury to cardiac myocytes and its mechanism. Acta Pharmaceutica Sinica 2007;42(3):263–268.

[11] Wang HJ, Jiang YY, Wei XF, Huang H, Tashiro S, Onodera S. et al. Silibinin induces protective superoxide generation in human breast cancer MCF-7 cells. Free Radic Res 2010; 44(1):90–100.

[12] Wang HJ, Wei XF, Jiang YY, Huang H, Yang Y, Fan SM, et al. Silibinin induces the generation of nitric oxide in human breast cancer MCF-7 cells. Free Radic Res 2010;44(5): 577–584.

[13] Duan W, Jin X, Li Q, Tashiro S, Onodera S, Ikejima T. Silibinin induced autophagic and apoptotic cell death in HT1080 cells through a reactive oxygen species pathway. J Pharmacol Sci 2011;113(1):48–56.

[14] Baran CP, Zeigler MM, Tridandapani S, Marsh CB. The role of ROS and RNS in regulating life and death of blood monocytes. Curr Pharm Des 2004;10(8):855–866.

[15] Oyagbemi AA, Azeez OI, Saba AB. Interactions between reactive oxygen species and cancer: the roles of natural dietary antioxidants and their molecular mechanisms of action. Asian Pac J Cancer Prev 2009;10(4):535–544.

[16] Droge W. Free radicals in the physiological control of cell function. Physiol Rev 2002;82(1):47–95.

[17] Schwartz LM, Smith SW, Jones ME, Osborne BA. Do all programmed cell deaths occur via apoptosis? Proceedings of the National Academy of Sciences 1993;90(3):980–984.
[18] Elmore S. Apoptosis: a review of programmed cell death. Toxicol Pathol 2007;35(4):495–516.
[19] Racz K, Feher J, Csomos G, Varga I, Kiss R, Glaz E. An antioxidant drug, silibinin, modulates steroid secretion in human pathological adrenocortical cells. J Endocrinol 1990; 124(2):341–345.
[20] Huang Q, Wu LJ, Tashiro S, Onodera S, Ikejima T. Silymarin-induced HeLa cell apoptosis in G0/G1 phase in serum-free medium. Chin J Clin Rehabil 2005;9(6):242–245.
[21] Mazumder S, Plesca D, Almasan A. Caspase-3 activation is a critical determinant of genotoxic stress-induced apoptosis. Methods Mol Biol 2008;414:13–21.
[22] Abu-Qare AW, Abou-Donia MB. Biomarkers of apoptosis: release of cytochrome c, activation of caspase-3, induction of 8-hydroxy-2'-deoxyguanosine, increased 3-nitrotyrosine, and alteration of p53 gene. J Toxicol Environ Health B Crit Rev 2001;4(3):313–332.
[23] Biederbick A, Kern HF, Elsasser HP. Monodansylcadaverine (MDC) is a specific in vivo marker for autophagic vacuoles. Eur J Cell Biol 1995;66(1):3–14.
[24] Seglen PO, Gordon PB. 3-Methyladenine: specific inhibitor of autophagic/lysosomal protein degradation in isolated rat hepatocytes. Proc Natl Acad Sci U S A 1982;79(6):1889–1892.
[25] Maiuri MC, Criollo A, Kroemer G. Crosstalk between apoptosis and autophagy within the Beclin 1 interactome. EMBO J 2010;29(3):515–516.
[26] Eruslanov E, Kusmartsev S. Identification of ROS using oxidized DCFDA and flow-cytometry. Methods Mol Biol 2010; 594:57–72.
[27] Mizushima N, Yoshimori T. How to interpret LC3 immunoblotting. Autophagy 2007;3(6):542–545.
[28] Debnath J, Baehrecke EH, Kroemer G. Does autophagy contribute to cell death? Autophagy 2005;1(2):66–74.
[29] Nezis IP, Shravage BV, Sagona AP, Johansen T, Baehrecke EH, Stenmark H. Autophagy as a trigger for cell death: autophagic degradation of inhibitor of apoptosis dBruce controls DNA fragmentation during late oogenesis in Drosophila. Autophagy 2010;6(8):1214–1215.
[30] Siwale RC, Yeboah GK, Addo R, Oettinger CW, D'Souza MJ. The effect of intracellular antioxidant delivery (catalase) on hydrogen peroxide and proinflammatory cytokine synthesis: a new therapeutic horizon. J Drug Target 2009;17(9):710–8.
[31] Komada F, Nishiguchi K, Tanigawara Y, Ishida M, Wu XY, Iwakawa S, et al. Protective effect of transfection with secretable superoxide dismutase (SOD) (a signal sequence-SOD fusion protein coding cDNA) expression vector on superoxide anion-induced cytotoxicity in vitro. Biol Pharm Bull 1997; 20(5):530–536.
[32] Li LH, Wu LJ, Tashiro S, Onodera S, Uchiumi F, Ikejima T. Silibinin prevents UV-induced HaCaT cell apoptosis partly through inhibition of caspase-8 pathway. Biol Pharm Bull 2006;29(6):1096–1101.
[33] Eisenberg-Lerner A, Bialik S, Simon HU, Kimchi A. Life and death partners: poptosis, autophagy and the cross-talk between them. Cell Death Differ 2009;16(7):966–975.
[34] Annovazzi L, Mellai M, Caldera V, Valente G, Tessitore L, Schiffer D. mTOR, S6 and AKT expression in relation to proliferation and apoptosis/autophagy in glioma. Anticancer Res 2009;29(8):3087–3094.
[35] Bui-Xuan N H, Tang PM, Wong CK, Fung KP. Photo-activated pheophorbide-a, an active component of Scutellaria barbata, enhances apoptosis via the suppression of ERK-mediated autophagy in the estrogen receptor-negative human breast adenocarcinoma cells MDA-MB-231. J Ethnopharmacol (2010):131(1):95–103.
[36] Sy LK, Yan SC, Lok CN, Man RY, CheCM. Timosaponin A-III induces autophagy preceding mitochondria-mediated apoptosis in HeLa cancer cells. Cancer Res 2008;68(24):10229–10237.
[37] Chen Y, Gibson SB. Is mitochondrial generation of reactive oxygen species a trigger for autophagy? Autophagy 2008;4(2): 246–248.
[38] Ricci JE, Gottlieb RA, Green DR. Caspase-mediated loss of mitochondrial function and generation of reactive oxygen species during apoptosis. J Cell Biol 2003;160(1):65–75.
[39] Janssen YM, Matalon S, Mossman BT. Differential induction of c-fos, c-jun, and apoptosis in lung epithelial cells exposed to ROS or RNS. Am J Physiol 1997;273(4 Pt 1):L789–796.
[40] Swanlund JM, Kregel KC, Oberley TD. Autophagy following heat stress: the role of aging and protein nitration. Autophagy 2008;4(7):936–939.
[41] Younce CW, Kolattukudy PE. MCP-1 causes cardiomyoblast death via autophagy resulting from ER stress caused by oxidative stress generated by inducing a novel zinc-finger protein, MCPIP. Biochem J 2010;426(1):43–53.
[42] Mira L, Silva M, Manso CF. Scavenging of reactive oxygen species by silibinin dihemisuccinate. Biochem Pharmacol 1994;48(4):753–759.
[43] Altorjay I, Dalmi L, Sari B, Imre S, Balla G. The effect of silibinin (Legalon) on the free radical scavenger mechanisms of human erythrocytes in vitro. Acta Physiol Hung 1992;80 (1–4):375–380.
[44] Kim KW, Choi CH, Kim T H, Kwon CH, Woo JS, Kim YK. Silibinin inhibits glioma cell proliferation via Ca2 + /ROS/ MAPK-dependent mechanism in vitro and glioma tumor growth in vivo. Neurochem Res 2009;34(8):1479–1490.
[45] Dewaele M, Martinet W, Rubio N, Verfaillie T, de Witte PA, Piette J, et al. Autophagy pathways activated in response to PDT contribute to cell resistance against ROS damage. J Cell Mol Med. 2010 Jul 7. Available:http://onlinelibrary.wiley.com/doi/10.1111/j.1582-4934.2010.01118.x/full via the INTERNET.
[46] Brookes PS, Yoon Y, Robotham JL, Anders MW, Sheu S-S. Calcium, ATP, and ROS: a mitochondrial love-hate triangle. Am. J. Physiol. Cell Physiol 2004;287:C817–C833.
[47] Zhou R, Yazdi AS, Menu P, Tschopp J. A role for mitochondria in NLRP3 inflammasome activation. Nature 2011;469 (7329):221–225.

This paper was first published online on Early Online on 25 October 2011